Peer-reviewed version available at *Energies* **2018**, *11*, 2374; doi:10.3390/en11092374

Article

Dimensional Analysis in Power Predicting of a Real Scale Wind Turbine Based on Wind Tunnel Torque Measurement of Small Scaled Models

Sutrisno Sutrisno [1,*], Sigit Iswahyudi [1,2] and Setyawan Bekti Wibowo [1,3]

[1] Department of Mechanical and Industrial Engineering, Faculty of Engineering, Universitas Gadjah Mada, Yogyakarta 55281, Indonesia; sutrisno@ugm.ac.id
[2] Department of Mechanical Engineering, Universitas Tidar, Magelang 56116, Indonesia; sigit.iswahyudi@untidar.ac.id
[3] Department of Mechanical, Vocational School, Universitas Gadjah Mada, Yogyakarta 55281, Indonesia; setyawanbw@ugm.ac.id
* Correspondence: sutrisno@ugm.ac.id; Tel.: +62-896-2266-9341

Abstract: A preliminary study of a wind turbine design is carried out using a wind tunnel to obtain its aerodynamic characteristics. Utilization of data from the study to develop large-scale wind turbines requires further study. This paper aims to discuss the use of wind turbine data obtained from the wind tunnel measurements to estimate the characteristics of wind turbines that have field size. The torque of two small-scale turbines was measured inside the wind tunnel. The first small-scale turbine has a radius of 0.14 m and the second small turbine has a radius of 0.19 m. Torque measurement results from both turbines were analyzed using Buckingham π theorem to obtain a correlation between torsion and diameter variations. The obtained correlation equation is used to estimate the field measurement of turbine power with a radius of 1.2 m. The resulting correlation equation can be used to estimate the power generated by the turbine by the size of the field well in the operating area of the tip speed ratio of the turbine design.

Keywords: wind tunnel; enlarge design; Buckingham π theorem; torque-diameter correlation; estimated power; field size; 3-D blade; stall delay

1. Introduction

The study of wind turbine design performance can be done quickly using various computational fluid dynamics software. The results of the study can be used as a basis to realize the design because the measurement results using software is relatively accurate. However, real measurements are needed because the conditions used in computing are ideal conditions while real conditions may differ considerably.

The research development progress in wind turbine technology is growing rather slowly in the last decades. Early mathematical works, started by Prandtl and also Joukowsky, were developed further by Kuchemann. He calculated the span and chord wise loading on straight and swept wings at subsonic speeds [1]. The concepts were deepened and sharpened for example with Goldstein's circulation function for optimal rotors with a hub, blade design and the influence of tip correction on rotor performance and actuator discs with swirl [2-5].

Lutz describes the practicality of lifting-line theory, Ayati calculates aerodynamic effects on wind turbine blades using the lifting-line theory, and digitally Lamar, developing a modified Multhopp approach for predicting lifting pressures and camber shape for composite planforms [6-8]. Moreover, Sutrisno et al., using the lifting-line theory, modeled the performances of three-dimensional (3-D) wind turbine blade plate-models with helicopter-like propeller blade tips [9].

Kesler made a comparison between the experimental thrust and propeller thrust predicted by Prandtl's lifting line theory. Abedi developed a vortex filament method for aerodynamic loads on rotor blades, and de Oliveira et al. investigated how does the presence of a body effect to the performance of an actuator disk [10-12].

In design blade horizontal axis wind turbine (HAWT), Plaza et al. conducted a comparison between blade element method (BEM) and CFD results for Mexico rotor aerodynamics. Bai et al. investigated a 10 KW HAWT blade and aerodynamic design using numerical simulation. Chehouri et al. reviewed performance optimization techniques applied to wind turbines. Singh and Ahmed examined blade design and testing of small wind turbine rotor performance for low wind speed applications. Suzan checks radical innovations in wind turbine blade design. Velázquez et al. studied the design and experiments of 1 MW HAWT [13-18].

In implementing BEM for design, Schubel and Crossley investigated the wind turbine blade design. Lynch conducted advanced CFD methods for wind turbine analysis. Elfarra examined the design and optimization of winglet and twisted aerodynamic using CFD HAWT rotor blade: winglet and twist aerodynamic. Maniaci et al. investigated the experimental measurement and CFD model development of thick wind turbine airfoils with leading edge erosion. Perfilev examined an optimization methodology optimization methodology for wind turbine blade geometry. Lutz and Wagner analyzed numerical shape optimization of subsonic airfoil sections. Rahimi et al. investigated the validity of BEM for simulation of wind turbines in complex load cases and comparison with experiment and CFD [19-26].

To enrich the insights, we need to compare mathematical works and BEM with 3-D approximation theory to include consideration of stall delay, turbulence, and separation. Sutrisno et al. studied the performance & flow visualization of three-dimensional (3-D) approximation theory of wind turbine blade. Sutrisno et al. learned the performances and stall delays of three-dimensional wind turbine blade plate-models with helicopter-like propeller blade tips. Sutrisno et al. investigated the rolled-up and tip vortices studies in the CFD model of the 3-D swept-backward wind turbine blades. Brocklehurst and Barakos reported a tip shapes review of helicopter rotor blade [9,27-29].

In HAWT stall delay, Dumitrescu and Cardos reported inboard stall delay due to the rotation. Hu et al. investigated a study on stall-delay for HAWT. Lee and Wu learned an experimental study of stall delay on the blade of a HAWT using tomographic particle image velocimetry. Sicot et al. studied rotational & turbulence effects on wind turbine blade investigation of the stall mechanisms. Wu et al. concluded a study of the active turbulence structures during stall delay. Yu et al. examined and inserted into the separate flow and stall delay for HAWT. Yu et al. scrutinized an insight into the separate flow and stall delay for HAWT [30-35].

In the case of a stall, turbulence, and separation, Bak et al. analyzed the full-scale wind turbine test of vortex generators mounted on the entire blade. Yu et al. scrutinized an insight into the separate flow and stall delay for HAWT [36-38].

The 3-D approximation theory relied heavily on rolled-up vortex and Q criterion. Gursul et al. studied the unsteady aerodynamics of non-slender delta wings. Gursul et al. reviewed flow control mechanisms of leading-edge vortices. Chattot explained the effects of blade tip modifications on wind turbine performance using vortex model. Pavese et al. learned the design of a wind turbine swept blade through extensive load analysis. Shen et al. analyzed the aerodynamic shape optimization of non-straight small wind turbine blades. Adegas et al. observed a power curve of small wind turbine generators-laboratory and field testing [6,39-43].

Scientist introduced Q-Criterion to visualize the rolled-up vortex appearances. Calderon et al. analyzed 3-D measurements of vortex breakdown. Haller explained an objective definition of a vortex. Muscari et al. learning modeling of vortex dynamics in the wake of a marine propeller. Zhang and Wu observed the aerodynamic characteristics of wind turbine blades with a sinusoidal leading edge. Ibrahim and New reported flow separation control of marine propeller blades through tubercle modifications [44-48].

Cai et al. learned the design of an optimal wing-body configuration to delay the onset of vortex asymmetry [49,50]. Using CFD, Bangga et al. explained the effect of the computational grid on accurate prediction of a wind turbine rotor using delayed detached-eddy simulations. Kim studied aerodynamic design and performance analysis of multi-MW class wind turbine blade [51,52].

Shafiqur Rehman et al. have reported a review on horizontal axis wind turbine blade design methodologies for efficiency enhancement [53]. The efficiency of the wind turbines can be increased by reducing the cut-in-speed by modifying / redesigning the blades. The problem is tackled by identifying the optimization parameters such as power coefficient, energy cost, blade mass, and blade design constraints such as physical, geometric, and aerodynamic

Schubel and Crossley (Schubel and Crossley) reveal the blade design of wind turbines, exclusively with horizontal axis rotors, including theoretical maximum efficiency, propulsion, practical efficiency, HAWT blade design, and blade loads [19]. Manufacturers seek greater cost efficiency by exploiting the ability to scale the design, greater cost effectiveness through increased turbine size

Two small turbines torque measurement have been conducted, and we used Buckingham π theorem to obtain a correlation between torsion and diameter variations. The correlation equation was developed and was used to estimate the field measurement of turbine power with a radius of 1.2 m. The resulting correlation equation can be used to estimate the power generated by the turbine by the size of the field well in the operating area of the ratio of the tip end of the turbine design.

The measurement of small-scale wind turbine models using wind tunnel is a commonly used way to obtain design characteristics. However, the data obtained require further analysis to be able to estimate the performance of wind turbines with sizes in the field. In this paper, dimensional analysis based on Buckingham theorem π is used to estimate the power to be generated by wind turbines with an actual scale based on torque correlations with changes in diameter of measurement results in the wind tunnel.

In this work, we considered the lifting-line theory in the form of simple mathematical works. Some practical implementation of BEM calculation was employed. We also considered the 3-D approximation theory, the flow visualization, the appearance of stall delay, rolled-up vortex phenomenon. Q-criterion rolled on CFD was implemented.

2. Wind turbine characteristics

2.1. Wind Turbine Scaling, Rule of similarity and Buckingham π Theorem

We executed the work started with the rule of similarity and Buckingham π theorem. The significant parameters that govern the rotor characteristics can be formulated as a function of turbine diameter [54]. In this study, all geometrical parameters of the blade are scaled linearly.

Following the Buckingham π theorem, the number of dimensionless parameters (Np) needed to correlate associated data equals the total number of variables (Nv) minus the number of independent dimensions needed to describe the problem (Nd) (Eq. 1) [55].

$$N_p = N_v - N_d, \tag{1}$$

For any associated dimensional quantity Q,

$$[Q] = [Q_0] \prod_{i=1}^{N_p-1} [P_i]^{a_i}, \tag{2}$$

Q_0 has the same dimension as Q. If $P_0 \equiv Q/Q_0$ is defined as a dimensionless quantity, then P_is as π factor are dimensionless. In Eq. 2, a_is are coefficients that must be determined.

2.2. Torque-Diameter Correlation

The elementary quantities used in the experiment variables could be mass (M), length (L) and/or

time (T). Experiment variables consist of five parameters, i.e., torque τ (ML2T-2), air density ρ (ML-3), wind speed U (LT-1), rotation speed RPM (T-1), and rotor diameter D (L). From the dimensional analysis, the correlation of torque and rotor diameter could be written as in Eq. 3.

$$[\tau] = \left[\frac{\rho U^5}{RPM^3}\right]\left[\frac{RPM.D}{U}\right]^{\alpha}, \quad (3)$$

From Eq. 3, we found that

$$P_0 = \tau_0 = \frac{RPM^2\tau}{\rho U^5}, \text{and } P_1 = \frac{RPM.D}{U},$$

3. Experimental Setup

3.1 Wind Turbine Design

In this study, one could use BEM procedures to design the geometries of the wind turbine blades. The rotors had three blades and applied airfoil NACA 4412 along with their span. The distributions of pitch angles and normalized chords length in spanwise were approximated using the BEM optimum distribution (Eq. 5 and 6) as depicted in Figure 1. The design used a tip speed ratio of 3.65. The calculated performance of the design is described in the form of power coefficient as a function of tip speed ratio as depicted in Figure 2. Figure 3 shows the three-dimension printed models that have a radius of 0.14 m.

$$\beta_r = \frac{2}{3}\text{atan}\left[\frac{1}{\lambda_D\left(\frac{r}{R}\right)}\right] - \alpha_D, \quad (4)$$

$$\left(\frac{c}{R}\right)_r = \frac{16\,\pi\left(\frac{r}{R}\right)_r}{C_{L,D}}\left\{\sin\left\{\frac{1}{3}\text{atan}\left[\frac{1}{\lambda_D\left(\frac{r}{R}\right)_2}\right]\right\}\right\}^2, \quad (5)$$

3.2 Parameters Measurement in wind tunnel

Figure 3 shows the schematic parameters of small-scale wind turbine measurement. The parameters consist of wind speed, the rotation speed of the rotor, and the torque of the rotor. A rope brake dynamometer system measured the torque. The torque was not measured directly. A balancing weight (W) was used to generate friction force on a pulley of Dp in diameter. The torque values were calculated from the difference between balancing weight and the values shown in digital balance (S) by Eq. (4).

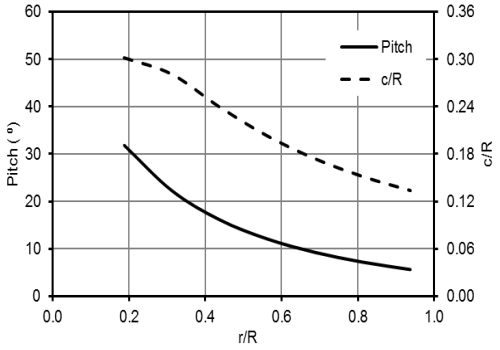

Figure 1. Designed pitch and normalized chords length in span wise.

Peer-reviewed version available at Energies 2018, 11, 2374; doi:10.3390/en11092374

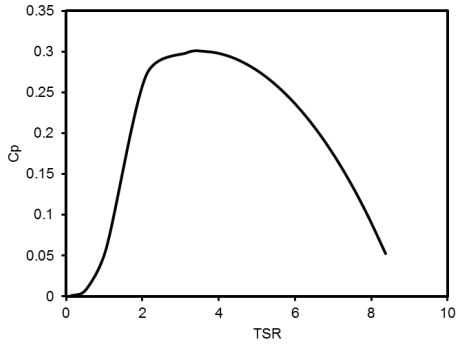

Figure 2. Calculated performance of the design was approximated by BEM

(**a**) (**b**)

Figure 3. Three dimensions printed of the rotors of radius 0.19 m. (**a**) The blade has a backward swept at its tip, (**b**) The blade has a helicopter head blade tip.

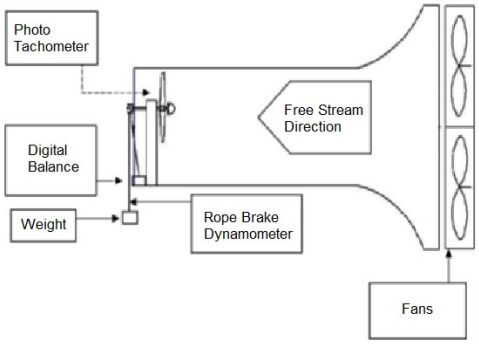

Figure 4. Test schematic in wind tunnel

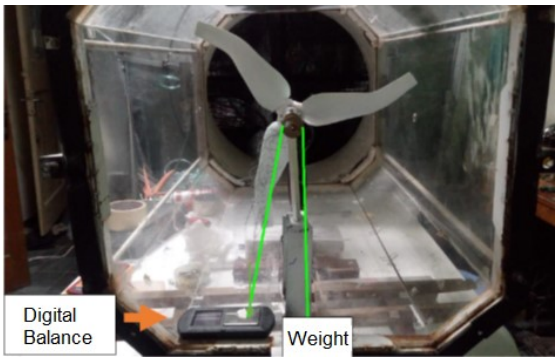

Figure 5. Measurement setup in wind tunnel

$$\tau = \frac{D_p}{2}(W - S), \tag{6}$$

3.3 Field measurement

Field measurement was done in the beach area (Figure 6). The location of the field was at the coastal line of Pantai Baru, Jogjakarta, Indonesia, about at a geographic location of 7.9894 S and 110. 2219 E. The tests were done by following the IEC 61400-12-1 standard.

Figure 6. Field measurement setup[56]

3.4. From BEM to 3-D wind turbine blade concept

Since the early research development of the wind turbine rotor theory, the wind turbine blade was divided into a number of independent span wise sections and the induced velocities could be calculated. This method for infinitely many blades was called the blade element momentum (BEM) theory.

At the moment, the concept slightly shifts, as an analogy of an airplane at first use planar wing, then implement swept wing. The wind turbine blade design, from using the BEM concept, and then shifts to the concept of 3-D wind turbines.

On the aircraft, an addition of swept on the wing, it slightly reduced performance but the stall was delayed, that high performance survived to higher angles of attack. As for wind turbines, with the addition of swept on the blade, it slightly reduces performance but stall is delayed, that the blade high performance will survive, to higher wind speeds. In wind turbine blades, since stall propagation from the root outward, swept positive/backward is from the root toward the tip [9], as seen in Fig, 3. This is very beneficial for the region with lots of gusty winds. This concept could be called as the 3-D wind turbine blade concept.

4. Results and Discussion

4.1 Measurement Result and Torque-Diameter Correlation

Figures 7 and 8 show the results of the torque measurement of small scaled rotors in the wind tunnel. The measured data then were evaluated by Eq. (3). Figure 9 shows the plotted non-dimensional torque (P_0) as a function of another non-dimensional parameter (P_1). Figure 9 indicates two region of data group. The first is data that forms relatively linear in logarithmic of P_0 axis and the second forms the non-linear. A correlation of torques associated with diameters of wind turbine rotors could be created using data in the linear region as stated in Eq. (7). The correlation would be chosen for estimating the power of field measurement of a wind turbine because of the nature of the generated power in the field would be similar with the region.

$$\frac{RPM^3\tau}{\rho U^5} = 0.0027\left(\frac{RPM.D}{U}\right)^{2.3385}, \quad (7)$$

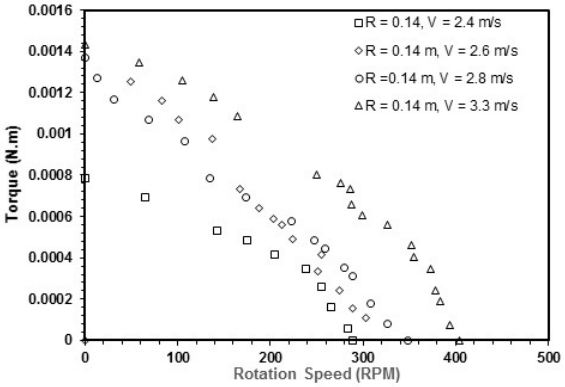

Figure 7. Torque measurement results of the rotor of radius 0.14 m

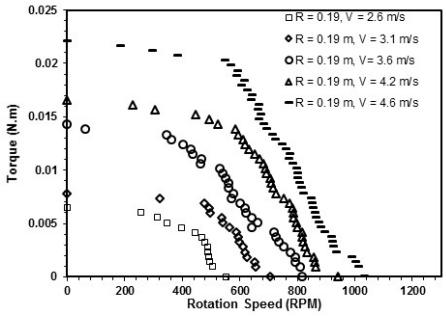

Figure 8. Torque measurement results of the rotor of radius 0.19 m.

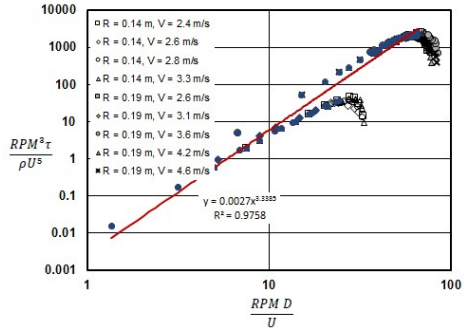

Figure 9. Correlated torque associated with rotor diameters.

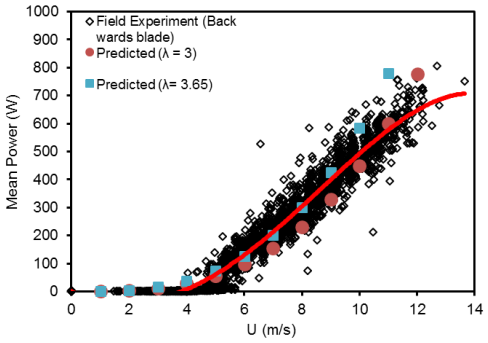

.

Figure 10. Results of power measurement of the rotor with a diameter of 2.4 m in the field [56] and predicted power values by data correlation from small-scaled rotors

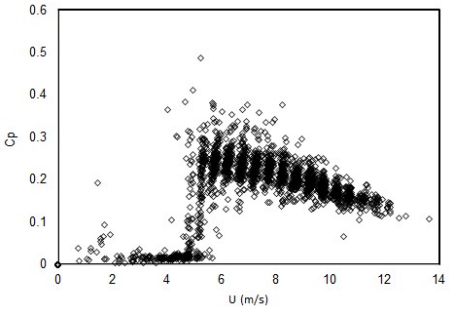

Figure 11. The altered power coefficient of field rotor by wind speed changes.

4.2 Field Measurement and Computed Power

Based on Eq. (7), the power of the rotor can be calculated using Eq. (8). The computed power with a selected tip speed ratio (λ) of 3.65 and 3 are shown in Figure 9.

$$P = 0.0027\left(\frac{RPM.D}{U}\right)^{8.8888}\frac{\rho U^3}{RPM^3}\frac{2\lambda U}{D}, \quad (8)$$

The results of the tests are described in Figure 10 [56]. Maximum standard deviation of the power of bin data in the field measurement is 161.5486 watt [56], whereas the error values from the correlation increases until 92.2884 watt at wind speed of 10 m/s. For wind speed greater than 10 m/s, the estimated power is higher than the expected values. The lower expected value at high wind speed might be caused by the rotor of the wind turbine rotates slower than the designed operation. Therefore, Eq. (6) would be confident enough to be used in estimating the results of the power measurement.

The correlation equation estimate that the power coefficient of the field rotor will be 0.21 constantly over all the ranges of the wind speed. The value is sound to be used in practical but with the correction of the ranges of the wind speed. Figure 11 describes the computed power coefficient based on field power measurement as a function of wind speed. Based on Figure 11, it is reasonable if the power coefficient of the rotor is estimated to be 0.21 in the range of wind speed form 5 m/s to 12 m/s.

For the results comparison between the lifting line theory and measured power, in the previous report[9], we have compared between performance coefficient (C_P) versus tip speed ratio (λ) implementing lifting line theory based on the Pistolesi principle with rotation, versus the actual measurement results. The matching result was satisfactory.

4.3 Flow visualization, rolled-up vortex, and Q-criterion

Figure 12 shows comparisons between the tuft patterns of backward wind turbine blades of radius r = 19 cm. The coefficient of performance of these two backward blades, since they both have the same styles, are similar[9]. Figure 12 showed the patterns at a) U=4.5 m/s, RPM=840, TSR=3.712, with weak stall pattern, b) U=5.2 m/s, RPM=1060, TSR=4.054, with half stall pattern, c) U=5.5 m/s, RPM=1120, TSR=4.059, similarly with half stall pattern, and the second row at d) U=3.0 m/s, RPM=200, TSR=1.325, with weak stall pattern, e) U=4.2 m/s, RPM=440, TSR=2.083, with half stall pattern, f) U=4.9 m/s, RPM=530, TSR=2.151, also with half stall pattern. It is clear that the blades have different shapes but give similar stall patterns

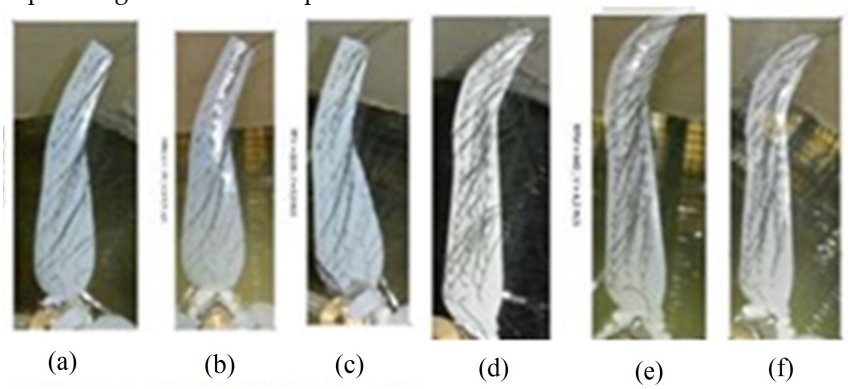

Figure 12. The flow visualization pattern comparison between the backward blade of radius r = 19 cm.

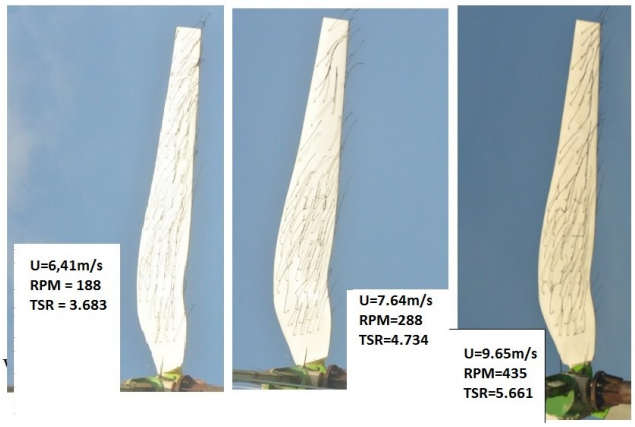

Figure 13. The flow visualization pattern of the backward blade of radius r = 120 cm, where a), with weak stall pattern, b) with half stall pattern and c) with stall to tip pattern, referred to [27].

It can be noted from Figure 12 that the first row, when the RPM is high as the wind speed is high, their patterns are similar to the second row where the RPM is rather low as the wind speed is also rather low, since their load are similar. Compared to Figure 13, they have similar patterns, even though the wind speed is high blowing upon bigger blades, but since they operate at similar TSR, they have similar pattern, since the load are adjusted to maintain the operating voltage, for electrical security.

5. Conclusion

Method selection in making experiment data of small-scale wind turbine valuable for designing large scale one is an important task. In this paper, dimensional analysis based on Buckingham π theorem work well to be applied. The pattern of the torque data that come out from a small-scale wind turbine test in the wind tunnel was made. Based on the results, the correlation of the torque data of small rotor associated with rotor diameter could be used to predict the result of field power measurements of the large one confidently as the errors are lower than the expected from the field measurement error.

The discussion in this paper is limited to rotor scaling up to 8.57. The use of Buckingham π theorem gives good result. An extending investigation is needed to study the effectiveness of the method if it be applied for higher scaling. One can also conclude that the lifting line theory supported the similarity character of the theory and its real measurement result, and tuft patterns of the backward wind turbine blade supported the similarity of the flow visualization pattern between small-scale and large-scale wind turbines.

Author Contributions: Conceptualization, Sutrisno; Methodology, Sutrisno and Sigit Iswahyudi; Software, Setyawan B. Wibowo; Validation, Sutrisno, Sigit Iswahyudi and Setyawan B. Wibowo; Formal Analysis, Sigit Iswahyudi; Investigation, Sigit Iswahyudi; Resources, Setyawan B. Wibowo; Data Curation, Setyawan B. Wibowo; Writing-Original Draft Preparation, Sutrisno and Sigit Iswahyudi; Writing-Review & Editing, Sutrisno, Sigit Iswahyudi and Setyawan B. Wibowo; Visualization, Setyawan B. Wibowo; Supervision, Sutrisno.; Project Administration, Sutrisno; Funding Acquisition, Sutrisno.

Funding: This research was funded by the Department of Mechanical & Industrial Engineering, Universitas Gadjah Mada, Indonesia, under the contract 1560/H1.17/TMI/LK/2016.

Acknowledgments: The authors would like to express sincere gratitude to Prof. Dr. Noer Ilman, Dr. Prajitno for the time spent in serious discussion, helpful suggestions, and useful conceptual contribution. We would like to thank also our students Farhan, Fadhil, Hasan, the laboratory staff members, Waji and Min, for giving their help in construction work and conducting data management, which we gratefully acknowledge.

Conflicts of Interest: The authors declare no conflict of interest. The funders had no role in the design of the study; in the collection, analyses, or interpretation of data; in the writing of the manuscript, and in the decision to publish the results.

Nomenclature

α_D : angle of attack of airfoil (design)
β_r : twist angel of airfoil
λ, λ_D : tip speed ratio
ρ : air density (kg/m3)
τ : torque (Nm)
a : constant
c : chord lenght (m)
r : radius (m)
$C_{L,D}$: coefficient of lift (design)
D : rotor diameter (m)
D_p : diameter of pulley
L : length
M : mass
N : total number of dimensionless parameters
P : computing power (W)
P_i : Buckingham π factor
Q : dimension quantity
RPM : rotation speed
S : digital balance
T : time (s)
U : wind speed (m/s)
W : balancing weight

References

1 Kuchemann, D. A Simple Method for Calculating the Span and Chordwise Loading on Straight and Swept Wings of any Given Aspect Ratio at Subsonic Speeds. **1956**, 2935, 1–53.
2 Okulov, V.L.; Sørensen, J.N.; Wood, D.H. The rotor theories by Professor Joukowsky : Vortex theories. *Progress in Aerospace Sciences*, **2014**, 1–28. DOI: 10.1016/j.paerosci.2014.10.002
3 Okulov, V.L.; Sørensen, J.N.; Shen, W.Z. Extension of Goldstein's circulation function for optimal rotors with hub. *Journal of Physics: Conference Series*, **2016**, 753, 022018. DOI: 10.1088/1742-6596/753/2/022018
4 Sørensen, J.N.; Okulov, V.L.; Mikkelsen, R.F.; Naumov, I. V; Litvinov, I. V. Comparison of classical methods for blade design and the influence of tip correction on rotor performance. *Journal of Physics: Conference Series*, **2016**,

753, 022020. DOI: 10.1088/1742-6596/753/2/022020

5 Van Kuik, G.A.M. Momentum theory of Joukowsky actuator discs with swirl. *Journal of Physics: Conference Series*, **2016**, 753, 022021. DOI: 10.1088/1742-6596/753/2/022021

6 Ayati, A.. Aerodynamic Effects on Wind Turbine Blades Using the Lifting-Line Theory. **2010**.

7 Lamar, J. A Modified Multhopp Approach for Predicting Lifting Pressures and Camber Shape for Composite Planforms in Subsonic Flow. [no date], m.

8 Lutz, T. Flugzeugaerodynamik II (Aicraft aerodynamics II). **2014**.

9 Sutrisno, S.; Deendarlianto, D.; Indarto, I.; Iswahyudi, S.; Bramantya, M.A.; Wibowo, S.B. Performances and Stall Delays of Three Dimensional Wind Turbine Blade Plate-Models with Helicopter-Like Propeller Blade Tips. *Modern Applied Science*, **2017**, 11, 189. DOI: 10.5539/mas.v11n10p189

10 R. Kesler. Propeller Thrust Analysis Using Prandtl's Lifting Line Theory, A Comparison Between The Experimental Thrust And The Thrust Predicted By Prandtl's Lifting Line Theory. **2014**.

11 Abedi, H. Development of Vortex Filament Method for Aerodynamic Loads on Rotor Blades. **2013**.

12 de Oliveira, G.; Pereira, R.B.; Ragni, D.; Avallone, F.; van Bussel, G. How does the presence of a body affect the performance of an actuator disk ? *Journal of Physics: Conference Series*, **2016**, 753, 1–11. DOI: 10.1088/1742-6596/753/2/022005

13 Plaza, B.; Bardera, R.; Visiedo, S. Comparison of BEM and CFD results for MEXICO rotor aerodynamics. *Jnl. of Wind Engineering and Industrial Aerodynamics*, **2015**, 145, 115–122. DOI: 10.1016/j.jweia.2015.05.005

14 Bai, C.J.; Hsiao, F.B.; Li, M.H.; Huang, G.Y.; Chen, Y.J. Design of 10 kW Horizontal-Axis Wind Turbine (HAWT) Blade and Aerodynamic Investigation Using Numerical Simulation. **2013**, 67, 279–287. DOI: 10.1016/j.proeng.2013.12.027

15 Chehouri, A.; Younes, R.; Ilinca, A.; Perron, J. Review of performance optimization techniques applied to wind turbines. *Applied Energy*, **2015**, 142, 361–388. DOI: 10.1016/j.apenergy.2014.12.043

16 Singh, R.K.; Ra, M. Blade design and performance testing of a small wind turbine rotor for low wind speed applications. *Renewable Energy*, **2013**, 50, 812–819. DOI: 10.1016/j.renene.2012.08.021

17 Tusavul, S.A. Radical Innovations in Wind Turbine Blade Design. **2014**.

18 Velázquez, M.T.; Vega, M.; Carmen, D.; Francis, J.A.; Pacheco, L.A.M.; Eslava, G.T. Design and Experimentation of a 1 MW Horizontal Axis Wind Turbine. *Journal of Power and Energy Engineering*, **2014**, 2014, 9–16.

19 Schubel, P.J.; Crossley, R.J. Wind turbine blade design. *Energies*, **2012**, 5, 3425–3449. DOI: 10.3390/en5093425

20 Faculty, T.A.; Lynch, C.E.; Fulfillment, I.P. Advanced cfd methods for wind turbine analysis. **2011**.

21 Elfarra, M.A. Horizontal Axis Wind Turbine Rotor Blade : Winglet and Twist Aerodynamic Design and Optimization Using Cfd a Thesis Submitted To the Graduate School of Natural and Applied Sciences of Middle East Technical University By Monier Ali Elfarra in Partial Fulfi. **2011**.

22 Baldacchino, D. *et al.* Experimental benchmark and code validation for airfoils equipped with passive vortex generators. *Journal of Physics: Conference Series*, **2016**, 753, 1–13. DOI: 10.1088/1742-6596/753/2/022002

23 Maniaci, D.C.; White, E.B.; Wilcox, B.; Langel, C.M.; van Dam, C.P.; Paquette, J.A. Experimental Measurement and CFD Model Development of Thick Wind Turbine Airfoils with Leading Edge Erosion. *Journal of Physics: Conference Series*, **2016**, 753, 022013. DOI: 10.1088/1742-6596/753/2/022013

24 Perfilev, D. Methodology for Wind Turbine Blade Geometry Optimization. **2013**.

25 Lutz, T.; Wagner, S. Numerical Shape Optimization of Subsonic Airfoil Sections. In: *European Congress on Computational Methods in Applied Sciences and Engineering ECCOMAS*. **2000**, 1–20.

26 Rahimi, H.; Hartvelt, M.; Peinke, J.; Schepers, J.. Investigation of the validity of BEM for simulation of wind turbines in complex load cases and comparison with experiment and CFD. *Journal of Physics: Conference Series*, **2016**, 749, 012015. DOI: 10.1088/1742-6596/749/1/012015

27 Sutrisno; Prajitno; Purnomo; B.W. Setyawan. The Performance & Flow Visualization Studies of Three dimensional (3-D) Wind Turbine Blade Models. *Modern Applied Science*, **2016**, 10. DOI: 10.5539/mas.v10n5p132

28 Sutrisno; Deendarlianto; Rochmat, T.A.; Indarto; Wibowo, S.B.; Iswahyudi, S.; Wiratama, C.; Erlambang, D.B.M. The Rolled-up and Tip Vortices Studies in the CFD Model of the 3-D Swept-Backward Wind Turbine Blades. *Modern Applied Science*, **2017**, 11, 118. DOI: 10.5539/mas.v11n12p118

29 Brocklehurst, A.; Barakos, G.N. A review of helicopter rotor blade tip shapes. *Progress in Aerospace Sciences*, **2013**, 56, 35–74. DOI: 10.1016/j.paerosci.2012.06.003

30 Dumitrescu, H.; Cardos, V. Inboard Stall Delay due to Rotation. *Journal of Aircraft*, **2012**, 49, 101–107. DOI: 10.2514/1.C031329

31 Hu, D.; Hua, O.; Du, Z. A study on stall-delay for horizontal axis wind turbine. *Renewable Energy*, **2006**, 31, 821–836. DOI: 10.1016/j.renene.2005.05.002

32 Lee, H.M.; Wu, Y. An experimental study of stall delay on the blade of a horizontal-axis wind turbine using tomographic particle image velocimetry. *Jnl. of Wind Engineering and Industrial Aerodynamics*, **2013**, 123,

56–68. DOI: 10.1016/j.jweia.2013.10.005

33 Sicot, C.Ã.; Devinant, P.; Loyer, S.; Hureau, J. Rotational and turbulence effects on a wind turbine blade . Investigation of the stall mechanisms. *Journal of Wind Engineering and Industrial Aerodynamics*, **2008**, 96, 1320–1331. DOI: 10.1016/j.jweia.2008.01.013

34 Wu, Y.; Mun, H.; Tang, H. A study of the energetic turbulence structures during stall delay. *International Journal of Heat and Fluid Flow*, **2015**, 54, 183–195. DOI: 10.1016/j.ijheatfluidflow.2015.05.013

35 Yu, G.; Shen, X.; Zhu, X.; Du, Z. An insight into the separate fl ow and stall delay for HAWT. *Renewable Energy*, **2011**, 36, 69–76. DOI: 10.1016/j.renene.2010.05.021

36 Ferreira, C. *et al.* Results of the AVATAR project for the validation of 2D aerodynamic models with experimental data of the DU95W180 airfoil with unsteady flap. *Journal of Physics: Conference Series*, **2016**, 753, 022006. DOI: 10.1088/1742-6596/753/2/022006

37 Bak, C.; Skrzypiński, W.; Gaunaa, M.; Villanueva, H.; Brønnum, N.F.; Kruse, E.K. Full scale wind turbine test of vortex generators mounted on the entire blade. *Journal of Physics: Conference Series*, **2016**, 753, 022001. DOI: 10.1088/1742-6596/753/2/022001

38 Schepers, G. Latest results from the EU project AVATAR : Aerodynamic modelling of 10 MW wind turbines. *Journal of Physics: Conference Series*, **2016**, 753, 022017. DOI: 10.1088/1742-6596/753/2/022017

39 Gursul, I.; Gordnier, R.; Visbal, M. Unsteady aerodynamics of nonslender delta wings. *Progress in Aerospace Sciences*, **2005**, 41, 515–557. DOI: 10.1016/j.paerosci.2005.09.002

40 Gursul, I.Ã.; Wang, Z.; Vardaki, E. Review of flow control mechanisms of leading-edge vortices. *Progress in Aerospace Sciences*, **2007**, 43, 246–270. DOI: 10.1016/j.paerosci.2007.08.001

41 Chattot, J.J. Effects of blade tip modifications on wind turbine performance using vortex model. *Computers and Fluids*, **2009**, 38, 1405–1410. DOI: 10.1016/j.compfluid.2008.01.022

42 Pavese, C.; Kim, T.; Murcia, J.P. Design of A Wind Turbine Swept blade Through Extensive Load Analysis. *Renewable Energy*, **2016**, 102, 21–34. DOI: 10.1016/j.renene.2016.10.039

43 Adegas, F.D.; Pena, G.D.M.; Antonio, J.; Alé, V.; Simioni, G.S. Power curve of small wind turbine generators–Laboratory and field testing. In: *RIO 3 - World Climate & Energy Event*. **2003**, 1–5.

44 Calderon, D.E.; Wang, Z.; Gursul, I. Three-dimensional measurements of vortex breakdown. *Experiments in Fluids*, **2012**. DOI: 10.1007/s00348-012-1317-1

45 Engineering, M.; Avenue, M. An objective definition of a vortex. **2005**, 525, 1–26. DOI: 10.1017/S0022112004002526

46 Muscari, R.; Di Mascio, A.; Verzicco, R. Modeling of vortex dynamics in the wake of a marine propeller. *Computers and Fluids*, **2013**, 73, 65–79. DOI: 10.1016/j.compfluid.2012.12.003

47 Zhang, R.-K.; Wu, V.D.J.-Z. Aerodynamic characteristics of wind turbine blades with a sinusoidal leading edge. *Wind Energy*, **2012**, 15, 407–424. DOI: 10.1002/we.479

48 Ibrahim, I.; New, T. Flow Separation Control of Marine Propeller Blades through Tubercle Modifications. In: *10th Pacific Symposium on Flow Visualization and Image Processing*. **2015**.

49 Han, C.; Kinnas, S.A. Study on the Wake Shape behind a Wing in Ground Effect Using an Unsteady Discrete Vortex Panel Method. *Open Journal of Fluid Dynamics*, **2013**, 3, 261–265. DOI: 10.4236/ojfd.2013.34032 Study

50 Cai, J.; Tsai, H.-M.; Luo, S.; Liu, F. Design of an Optimal Wing-Body Configuration to Delay Onset of Vortex Asymmetry. *AIAA Journal*, **2011**, 49, 164–171. DOI: 10.2514/1.J050595

51 Bangga, G.; Weihing, P.; Lutz, T.; Krämer, E. Effect of computational grid on accurate prediction of a wind turbine rotor using delayed detached-eddy simulations. *Journal of Mechanical Science and Technology*, **2017**, 31, 2359–2364. DOI: 10.1007/s12206-017-0432-6

52 Kim, B.; Kim, W.; Bae, S.; Park, J.; Kim, M. Aerodynamic design and performance analysis of multi-MW class wind turbine blade †. *Journal of Mechanical Science and Technology*, **2011**, 25, 1995–2002. DOI: 10.1007/s12206-011-0521-x

53 Rehman, S.; Alam, M.; Alhems, L.; Rafique, M. Horizontal Axis Wind Turbine Blade Design Methodologies for Efficiency Enhancement—A Review. *Energies*, **2018**, 11, 506. DOI: 10.3390/en11030506

54 Ashuri, T. Beyond Classical Upscaling : Integrated Aeroservoelastic Design and Optimization of Large Offshore Wind Turbines. **2012**. DOI: 10.4233/uuid:d10726c1-693c-408e-8505-dfca1810a59a

55 McDonough, J.M. *Lectures in Elementary Fluid Dynamics : Physics , Mathematics and Applications*. Lexington: University of Kentucky, **2009**.

56 Sutrisno; Iswahyudi, S.; Wibowo, S.B.; Kartika, W.; Qomar, F. Field Performance Measurement of Small-Scale Three-Dimensional (3-D) Wind Turbines. In: Pranoto, I. (ed.) *The 9th International Conference on Thermofluids*. Jogjakarta: AIP Publishing, **2017**.